BioNanoSci. (2013) 3:367–377
DOI 10.1007/s12668-013-0109-2

Partial Recovery of Silver Nanoparticle-Induced Neural Cytotoxicity through the Application of a Static Magnetic Field

Nicholas J. Braun · Kristen K. Comfort · John J. Schlager · Saber M. Hussain

Published online: 4 October 2013

Abstract Due to their tremendous antimicrobial properties, silver nanoparticles (AgNPs) have become incorporated into a number of consumer, industrial, and medical applications. However, AgNPs have also been shown to induce a strong cytotoxic response, brought on by an excess of cellular stress, which has severely limited the inclusion of AgNPs in nano-based biological applications, including drug delivery and bioimaging techniques. Previous investigations into magnetic field (MF) exposure have determined the potential of MFs to reduce the stress response in cellular systems; however, the ability of MF to protect cells from AgNPs has never been explored. As such, this study sought to identify if concurrent exposure to AgNPs and a 30-mT static MF could produce a diminishment of the cytotoxic and stress responses in a murine neural stem cell line (NE-4C). We discovered that the presence of MF provided a layer of protection from the negative AgNP effects, with a 15 % increase in viability noted up to a threshold concentration of 10 μg/mL. This partial recovery of AgNP-dependent cytotoxicity was found to correlate with increased ki67 expression and a substantial decrease in the NE-4C stress response including reactive oxygen species generation and NFκB and c-Jun expression. As neurological models are highly susceptible to stress, this study identified MF stimulation as a potential mechanism to counteract detrimental AgNP effects in neural cells, thereby demonstrating that a joint AgNP and MF system may be advantageous to progress neurological nano-based applications.

Keywords Silver nanoparticle · Static magnetic field · Cellular stress · Nanoparticle internalization · Neural cells

N. J. Braun · K. K. Comfort · J. J. Schlager · S. M. Hussain (✉)
Molecular Bioeffects Branch, Human Effectiveness Directorate, Wright Patterson AFB, Dayton, OH 45433, USA
e-mail: Saber.hussain@wpafb.af.mil

N. J. Braun
Department of Biomedical Engineering, Purdue University, West Lafayette, IN 47907, USA

K. K. Comfort
Department of Chemical and Materials Engineering, University of Dayton, Dayton, OH 45460, USA

1 Introduction

Due to their unique physicochemical properties, nanoparticles (NPs) have been incorporated into a large number of products and applications than span multiple sectors including consumer goods, military, and medicine. However, as the number of NP-based applications and products continue to grow, the potential hazards and effects associated with NP exposure must be thoroughly assessed and monitored. As such, it is crucial to develop a thorough understanding of how physiological systems respond and react to engineered NPs in an effort to maintain safe exposure levels and scenarios. In particular, the inclusion of silver nanoparticles (AgNPs) into common products and applications has exponentially grown due to their well-renowned antimicrobial and antibacterial properties [1]. AgNPs are heavily utilized in both consumer and medical products with specific examples including antimicrobial bandages and ointments, various types of clothing, food packaging, surgical tools, aerosol spray products, and personal hygiene products [2, 3].

Due to the prevalent and wide-reaching usage of AgNPs, it naturally follows that exposure levels to these nanosized particles are higher than ever before. This fact proves somewhat worrisome as multiple studies have demonstrated the ability of AgNPs to induce a strong cytotoxic response, brought on by augmented cellular stress and reactive oxygen species (ROS) production [4–6]. Beyond the well-investigated stress response, AgNP exposure has been shown to induce several other detrimental cellular effects, including interference in

signal transduction, gene modification, immune activation, and DNA damage [7–9]. Taken together, these bioresponses to AgNPs and increased exposure rates have warranted public health studies to analyze, model, and monitor the rate of AgNPs released into the environment [10]. Furthermore, recent investigations have determined that the root cause behind AgNP-dependent toxicity is the dissolution of the particles into silver ions [11, 12], of which the influence of external fields on this process has yet to be elucidated.

While the cellular impact of AgNPs has been extensively studied, to date, few investigations have focused on their influence in a neuronal cell model. However, one study identified the ability of AgNPs to increase the permeability of the blood–brain barrier (BBB), possibly allowing for their translocation into and dissemination throughout the brain [13]. Following passage through the BBB, AgNPs induced inflammation and neurotoxicity; an effect associated solely with AgNPs [13, 14]. These physiological consequences have the potential to induce serious ramifications, as neuronal stress has been linked to health concerns including memory loss, reduced cognitive performance, and Alzheimer's disease [15, 16]. Therefore, it is highly advantageous to identify a neuroprotective mechanism to control or minimize neuronal stress and inflammatory responses in order to allow for the development of NP-based applications including medical imaging techniques and drug delivery systems.

Paralleled to NPs, exposure to magnetic fields (MFs) has greatly increased in recent history due to technological advances and heightened production of personal electronics, electronic appliances, and power lines worldwide. Concerns for the potential health hazards associated with MF exposure are also rapidly increasing, leading to extensive investigation into bioeffects brought on by MF exposure, of varying intensities and types [17, 18]. These studies demonstrated that MF stimulation resulted in a reduction in cellular stress and an induction of gene modulation [19, 20], but the cellular response was variable and highly dependent on a number of factors including cell model, class of MF, and strength of MF. Although the mechanism behind the observed cellular response to MF exposure remains unclear, the effects have been well-documented and explored. The impact of MF application on cognition has also been a subject of interest, although meta-analyses of the data called for improvements in research design because of inconclusive data [21]. Furthermore, limited research has been conducted to evaluate cellular reactions under joint NP and MF exposure. Analogous to MF-dependent effects, simultaneous exposure scenarios have produced combinatorial effects that are both beneficial and detrimental to cellular systems [22–24], demonstrating the critical need to further explore this novel research niche. However, these studies indicated that the stress response was a common target of both MF and NP exposure indicating the potential for these stimuli to influence, and possibly counteract, one another in a physiological system.

As such, we sought to explore if the application of a static MF could successfully reduce the known AgNP-dependent cytotoxicity and stress activation in the neural NE-4C cell line. Owing to the increased developments and utilization of both NPs and MFs, concurrent exposure is a likely scenario, further motivating investigation into possible synergistic effects. We identified that a 30 mT static MF was able to partially counteract Ag-NP induced NE-4C cytotoxicity. However, this response was only observed at lower AgNP dosages with no discernible impact identified over concentrations of 10 μg/mL. The mechanism behind this response was further explored and found to be stimulated by MF-dependent reduction of the stress response as evaluated through multiple markers including ROS, c-Jun, and NFκB. This study established that the application of a static MF was able to partially counteract the stress and cytotoxic effects of AgNPs in neural cells providing a potential means for neurological protection during NP-based applications.

2 Materials and Methods

2.1 Nanoparticle Synthesis and Characterization

The citrate-stabilized AgNPs utilized in this experiment were purchased from Nanocomposix (San Diego, CA, USA) in solution form. Transmission electron microscopy (TEM) was performed on a Hitachi H-7600 microscope (Tokyo, Japan) to determine primary NP size and to verify spherical morphology. This analysis was performed on the AgNP stock solution with a concentration of 1 mg/mL. Dynamic light scattering (DLS) was used to evaluate NP agglomeration size and zeta potential analysis was used to assess surface charge, both on a Malvern Zetasizer Nano ZS instrument (Malvern, Worcestershire, UK). Both DLS and zeta potential analyses were carried out at a concentration of 50 μg/mL as per the manufacturer's recommendation. The spectral profile was visualized via UV–VIS on a Varian Cary 5000 also at 50 μg/mL. The degree of particle dissolution after 24 h at 37 °C in cell culture medium was evaluated by separation of released ions from the AgNPs through tangential flow filtration (Kros Flo Research System, Spectrum Labs) and silver content analysis on a Perkin Elmer NexION 300D inductively coupled plasma mass spectrometry (ICP-MS). This degree of ionic dissolution experimentation was performed at 5 μg/mL AgNPs

2.2 Cell Culture

The NE-4C (mouse neural stem cell) cell line was purchased from the American Type Culture Collection (ATCC, Manassas,

VA, USA) and was cultured in minimum essential medium (Eagle) supplemented with 10 % fetal bovine serum and 1 % penicillin–streptomycin (ATCC). The NE-4C cells were grown on culture dishes coated with 15 μg/mL poly-L-lysine for optimized adherence and proliferation and maintained at 37 °C and 5 % CO_2. During experimentation, cells were seeded into poly-L-lysine-coated 6 or 96-well culture plates or two-well chambered slides (Fisher Scientific, Pittsburg, PA, USA). Immediately before cellular exposure, AgNPs were diluted to the denoted concentration in NE-4C media and vortexed to ensure uniformity and minimize agglomeration.

2.3 Magnetic Field Exposure

NE-4C cells were exposed to a static MF generated by a high-temperature ferrite permanent bar magnet (McMaster-Carr, Cleveland, OH, USA). For MF stimulation, the cell culture plate was placed directly on top of the magnet and situated within an incubator. A diagram illustrating the central placement of the cell plates and utilized magnet is shown in Fig. 1. Control groups underwent the same experimental protocol but incurred no MF stimulation beyond the normal gravitational MF of approximately 0.05 mT. Control groups were kept in a separate incubator to ensure no unintentional MF exposure from the permanent magnets.

The physical dimensions of the magnet were 152×10.2×13 mm and a centralized location on the magnet was defined in order to ensure equable MF strengths and exposure. The MF strength in this centralized area was quantified through the utilization of a LakeShore 410 Gaussmeter with a transverse Hall probe (Westerville, OH, USA). The probe was placed a distance of 4 mm above the magnet surface to account for the height that the cells would be resting at within their plate. The magnetic flux within the allotted cell placement region was recorded 20 times and averaged, yielding MF strength of 31.3 ±0.23 mT; hereafter, referred to as 30 mT. Based on this analysis, it can be concluded that although the MF lines are by definition inhomogeneous in direction and strength, the cellular exposure region was small enough to generate constant MF exposure, within 1 % accuracy.

2.4 Cytoviva Imaging

Cells were seeded in a two-chambered slide at a concentration of 1×10^5 cells/chamber and left to incubate for 24 h. After incubation, the cells were dosed with AgNPs at a concentration of 5 μg/mL and exposed to the predetermined MF conditions and placed in incubation for 24 h. Cells were then fixed with 4 % paraformaldehyde and incubated with Alexa Fluor 555-phalloidin (Invitrogen, Carlsbad, CA, USA) for actin staining and DAPI (Invitrogen) for nuclear staining. The slides were sealed, followed by imaging using a CytoViva 150 ultraresolution attachment on an Olympus BX41 microscope (Aetos technologies, Auburn, AL, USA).

2.5 Cellular Viability

The viability of the NE-4C cells was assessed using the CellTiter 96 Aqueous One Solution (Promega, Madison, WI, USA) which evaluates mitochondrial function. Cells were seeded into a poly-L-lysine coated 96-well plate at a concentration of 7,500 cells/well and incubated for 24 h, after which the cells were exposed to the stated AgNP and MF conditions. After 24-h exposure to the stated conditions, the cells were washed and viability was assessed as per the manufacturer instructions using a SpectraMAX Gemini Plus microplate reader (Molecular Devices, Sunnyvale, CA, USA). An initial absorbance reading was also performed to account for background interference from the presence of AgNPs. NE-4Cs left untreated served as the negative control and cells exposed to silver nitrate were the positive control.

2.6 Reactive Oxygen Species Production

The fluorescent probe dichlorofluorescein diacetate (DCFH-DA, Invitrogen) was used as a means of monitoring the ROS

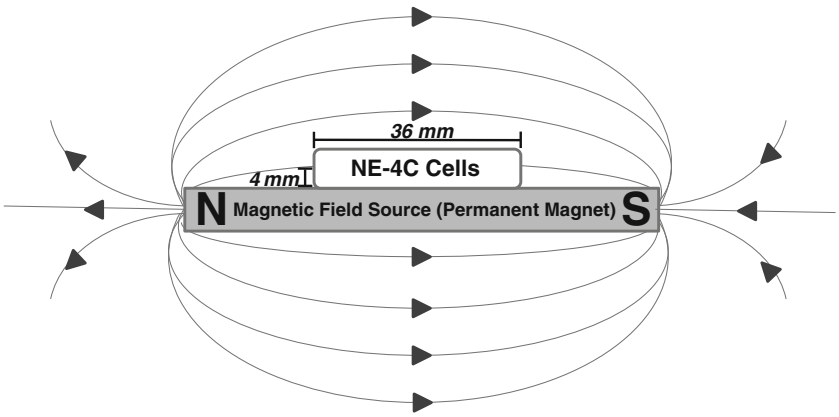

Fig. 1 Static magnetic field exposure system. A ferrite permanent magnet was utilized as a means for exposing NE-4C cells to a static MF. The cells were placed directly over the magnet which was situated within an incubator and produced a field strength of approximately 30 mT at the height equivalent to the cellular level

being produced by cells. NE-4C cells were seeded at a density of 7,500 cells/well in poly-L-lysine coated 96-well plates and incubated for 24 h. After incubation, cells were washed and 100 μL of 100 μM DCFH-DA was added for 30 min. The probe was then washed out, followed by introduction of the denoted AgNP and MF experimental conditions. The cells were returned to the incubator and at predetermined time points underwent spectrophotometric analysis on a SpectraMAX Gemini Plus microplate reader. Wells without AgNPs or MF exposure acted as a negative control, while cells dosed with hydrogen peroxide served as a positive control for ROS production.

2.7 Antibody Staining and Fluorescence Evaluation

In a 96-well plate NE-4Cs cells were seeded at a density of 7,500 cells/well the day before experimentation. They were then dosed with the denoted AgNP and MF conditions for 24 h, followed by preparation for fluorescence evaluation [25]. Briefly, cells were washed, fixed with 4 % paraformaldehyde (Sigma Aldrich), permealized with 1 % Triton-X100 (Thermo Scientific), and blocked with 1 % bovine serum albumin (Thermo Scientific). The NE-4Cs were then probed with the targeted primary and secondary antibodies, and the fluorescence was measured on a SpectraMAX Gemini Plus microplate reader. Primary antibodies were used to evaluate ki67, NF-κB, and c-Jun with the appropriate corresponding secondary antibodies (Thermo Scientific).

2.8 Silver Nanoparticle Uptake

NE-4C cells were seeded in a six-well plate at a density of 5×10^5 cells/well and allowed to incubate for 24 h. Cells were then dosed with AgNPs at a concentration of 5 μg/mL and incubated for an additional 24 h under the stated MF exposures. The cells were then washed, detached with trypsin, counted, and digested with an aqueous solution of 0.05 % Triton X-100, 3 % HCl, and 1 % HNO3. The amount of intracellular silver was then quantified through ICP-MS on a Perkin Elmer NexION 300D (Waltham, MA, USA).

2.9 Statistical Analysis

All data presented is expressed as the mean±the standard error of the mean. A one-way ANOVA with Bonferroni post-test was run with Graph Pad Prism (La Jolla, CA, USA) to determine statistical significance. An asterisk denotes a p value of ≤0.05, indicating significance between 0 and the 30 mT MF exposure conditions.

3 Results and Discussion

3.1 Nanoparticle Characterization

In addition to having different characteristics from their bulk counterparts, the bioeffects and cytotoxic response caused by NPs are strongly influenced by changes in the physical properties of the NPs themselves. As such, extensive characterization of NPs before introducing them into physiological systems is essential in understanding the nature of the cellular response [26]. Therefore, the AgNPs used in this study underwent an array of characterization assessments including determination of primary NP size, verification of spherical morphology, evaluating the extent of agglomeration, surface charge evaluation, rate of ionic dissolution, and identification of the AgNP spectral signature. The results of these characterization assessments are presented in Table 1 and Fig. 2.

One property that has been shown to play a significant role in the determination of cytotoxicity of NPs is their primary size [27]. TEM imaging was utilized to determine the primary size of the AgNPs used in this study, which was calculated to be 10.05±0.71 nm (Fig. 2a, Table 1). Next, UV–VIS demonstrated the characteristic AgNP peak at 400 nm and complimented the uniform particle quality seen in TEM images through identification of a sharp spectral signature (Fig. 2b). Previous studies have demonstrated that all nanomaterials will agglomerate to some degree when in solution due to their surface chemistries, interparticle interactions, and thermodynamic properties [28]; this property can be thought of as the effective NP size. DLS was used to quantify the approximate agglomerate size of the 10 nm AgNPs following dispersion in both media and water, and as expected, a larger effective size was observed in the media (Table 1). This increase is due to the protein binding to the NP surface, creating a corona or shell around the particle that has been found to modulate both interparticle interactions and the nanocellular interface [29, 30].

However, one major limitation of DLS is that it can provide an agglomerate size, but does not definitively identify the shape of the NP agglomerates. Typically, NPs will want to form an aggregate in the lowest entropy state, which is a sphere, but that is not always the case. One way to qualitatively assess the shape is through the polydispersity index (PDI), which is a measure of the uniformity or heterogeneity of the NP sample. A low PDI, generally less than 0.3, indicates excellent particle uniformity and size agreement whereas a high PDI denotes varying agglomerate sizes and a heterogeneous sample. As the DLS is designed for spherical particles, any nonspherical morphology will produce a high PDI value due to equipment-detecting multiple dimensions such as length and width of a nanorod. Therefore, as the PDIs associated with the AgNPs utilized in this study are all low, in both water and media, it is supportive of the claim that the

Table 1 Silver nanoparticle characterization

Primary size (nm)	Agglomerate size (nm)			Zeta potential (mV)			Ionic dissolution (%)	
10.1±0.7	Water	Media (−MF)	Media (+ MF)	Water	Media (−MF)	Media (+ MF)	Media (−MF)	Media (+ MF)
	40.6±0.2	60.9±0.3	66.8±0.1	−22.8±0.7	−12.4±0.5	−12.1±1.6	0.38±0.08	0.33±0.05
	PDI: 0.23	PDI: 0.17	PDI: 0.28					

aggregates are globular or spherical in nature. Furthermore, the impact of the 30 mT MF on the degree of AgNP agglomeration was of considerable interest as MF has the ability to modulate agglomeration patterns. When under the influence of MF for 24 h, a slight increase in the degree of AgNP aggregation was identified, but was less than a 10 % change from the 0 mT condition. Moreover, the PDI values associated with the AgNPs under MF influence remained under the 0.3 threshold, suggesting that no significant alterations to agglomerate shape occurred.

It is also important to ascertain the surface charge, or zeta potential, as charge has been shown to dictate protein binding to the NP surface and resultant cytotoxicity [31]. The results of the zeta potential analyses are shown in Table 1 and demonstrated a negative surface charge, which is due to the citrate coating on the AgNPs. Furthermore, the presence of MF did not alter the surface charge. As the rate of ionic dissolution of AgNPs has been strongly linked to the observed cellular responses, the next step was to ascertain the quantity of silver ions produced in media both with and without the presence of MF. From Table 1, it can be seen that the application of MF did not significantly alter the rate of dissolution, indicating that observed modifications are not due to a modification of ion production. Taken together, these characterization results suggest that the presence of MF induced minimal changes to the physical properties and behavior of the AgNPs.

3.2 Assessment of AgNP Interactions with NE-4Cs under MF Exposure

Next, fluorescence microscopy was utilized to qualitatively assess the interactions between the NE-4C cells and AgNPs, also known as the nanocellular interface (Fig. 3). This was important to determine as alterations to morphology and nanocellular interactions have been correlated to observed cytotoxicity and bioeffects. In contrast with previous studies [32], exposure to the 30 mT MF did not induce a significant morphological alteration in NE-4C cells, as seen in Fig. 3a,b. However, when 1 μg/mL of AgNPs were introduced to the cells, a significant amount of actin inflammation and disorganization was observed, which is indicative of augmented cellular stress (Fig. 3c) [33]. When NE-4Cs were concurrently exposed to AgNPs and MF, it appears that there is a reduction in the degree of actin disorganization (Fig. 3d) indicating that the MF is able to partially diminish that response in agreement with previous data that indicated stress as a target for MF [23].

Furthermore, in both cases of AgNP exposure, the AgNPs are seen strongly associating with the NE-4C cells, indicating that the MF does not disrupt the response of nanocellular cellular interactions. In addition, it can be noted that the AgNPs do not cluster together in the same manner that magnetic particles do when exposed to a static MF [23] indicating that magnetic properties, or lack thereof, of silver do not change significantly on the nanoscale. In corroboration with characterization data, these observations strengthen the argument that the presence of a static MF did not alter the properties or behavior of the AgNPs used in the study. As such, any biological alterations discovered in NE-4Cs during concurrent exposure are due to the combinatorial AgNP and MF effects on the cells and not the ability of MF to alter AgNP behavior.

However, at this point, it is critical to discuss the role that the stabilizing agent during synthesis and the surface functionalization play in defining the nanocellular interface. Surfactant or stabilizing agents are critical to the reproducible

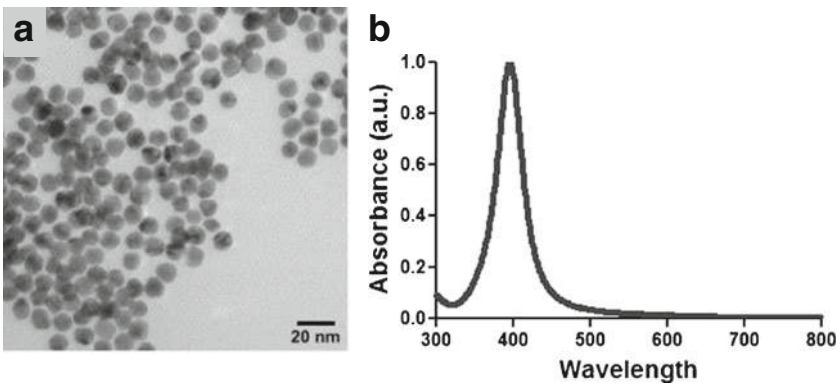

Fig. 2 Silver nanoparticle characterization. **a** Representative TEM images demonstrate the spherical morphology and approximate 10-nm primary size of the AgNPs utilized in this study. **b** The spectral signature of the AgNPs demonstrated the characteristic silver peak at 400 nm and no impurities

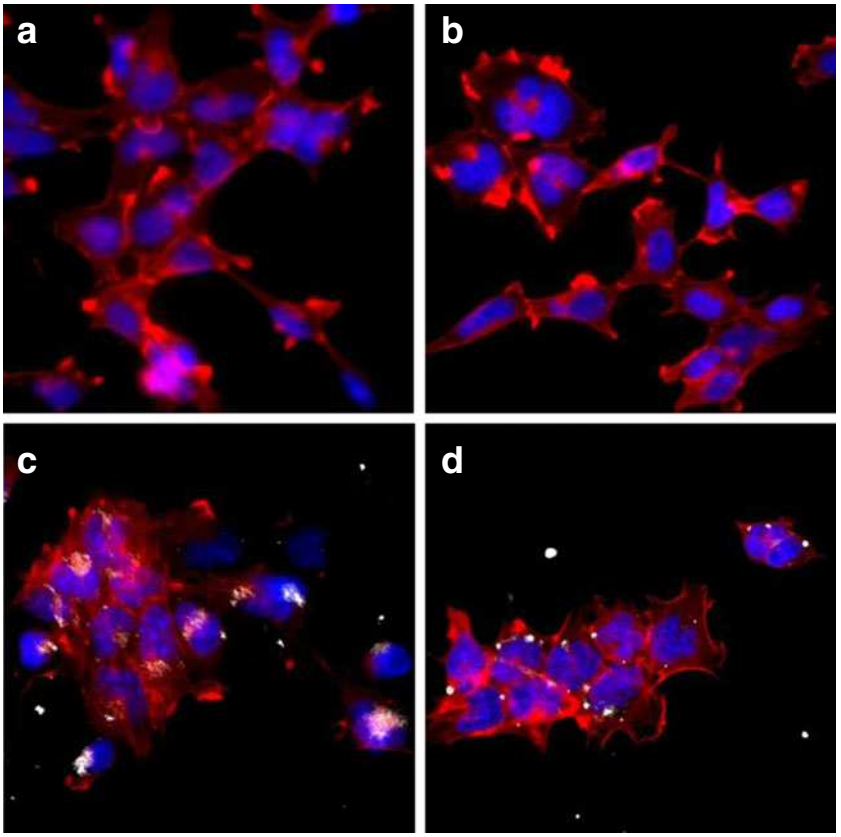

Fig. 3 CytoViva evaluation of the nanocellular interface. The influence of a 30 mT static MF on the interactions between AgNPs and NE-4Cs was examined through high-resolution fluoresce microscopy. Following 24 h of exposure representative images are shown for the experimental conditions of **a** 0 μg/mL AgNP and 0 mT, **b** 0 μg/mL AgNP and 30 mT, **c** 1 μg/mL AgNP and 0 mT, and **d** 1 μg/mL AgNP and 30 mT. The NE-4C cells underwent actin (*red*) and nuclear (*blue*) staining with metallic NPs reflecting *white*

and uniform synthesis of NPs; however, this produces particles with different surface functionalizations and coatings. Furthermore, the nature and concentration of the stabilizer is able to directly control the final morphology of the nanomaterials, again introducing variability. Both the surface chemistry and the particle shape of the particles dictates the mechanisms through which the NPs interact with the cells and the resultant nanocellular interface. Therefore, the mode of AgNP synthesis has the potential to directly impact both the interface as well as MF influence on this boundary. So while we identified no discernible difference in the way AgNPs interact with the cellular environment under the influence of MF, this may not be the case for all nanomaterials. This highlights the need to expand investigations into concurrent NP and MF exposure to produce a more fundamental understanding of potential synergistic effects.

3.3 Influence of NE-4C Cellular Viability by AgNPs and MF

As previously mentioned, AgNPs are renowned for their high levels of induced cytotoxicity and harmful bioeffects. However, assessing the impact of a static MF on a biological system has been somewhat more elusive. Depending on the cell line being examined, both proliferative and apoptotic effects have been observed with mixed results [34]. Without MF exposure, a traditional dose-dependent cytotoxic response was seen with the AgNPs as expected (Fig. 4a). Stimulation with the static MF alone resulted in an approximate 15 % increase in NE-4C viability, demonstrating its potential for a proliferative effect. However, upon concurrent exposure, it was found that the MF was able to partially recover AgNP-induced cytotoxicity (~15 %) up to a concentration of 5 μg/mL. The ability of MF to partially recover AgNP-induced cytotoxicity was also explored after a duration of 48 h and found to be similar (data not shown) indicating that time is not a predominant factor in this response. Due to the dramatic cytotoxic response observed at 25 μg/mL, we wished to explore intermediate AgNP concentrations to further investigate the recovery kinetics during co-exposure (Fig. 4b). With a 10 μg/mL AgNP concentration, a similar MF-dependent recovery effect was observed; however, above that dosage, the MF had no significant impact on NE-4C viability. Interestingly, this phenomenon appears to have a clear breakpoint occurring at 10 μg/mL AgNP exposure, after which the MF is incapable of rescuing cytotoxicity. This is likely due to the fact that the innate antioxidant and antistress ability of the NE-4Cs is overwhelmed by the AgNPs at this breakpoint concentration.

Ki67 is a recognized marker for cell proliferation and growth [35] and was quantified to verify the MF-dependent proliferative results observed. As expected, the presence of AgNPs decreased the ki67 expression as concentration increased, correlating with a reduction in NE-4C proliferation.

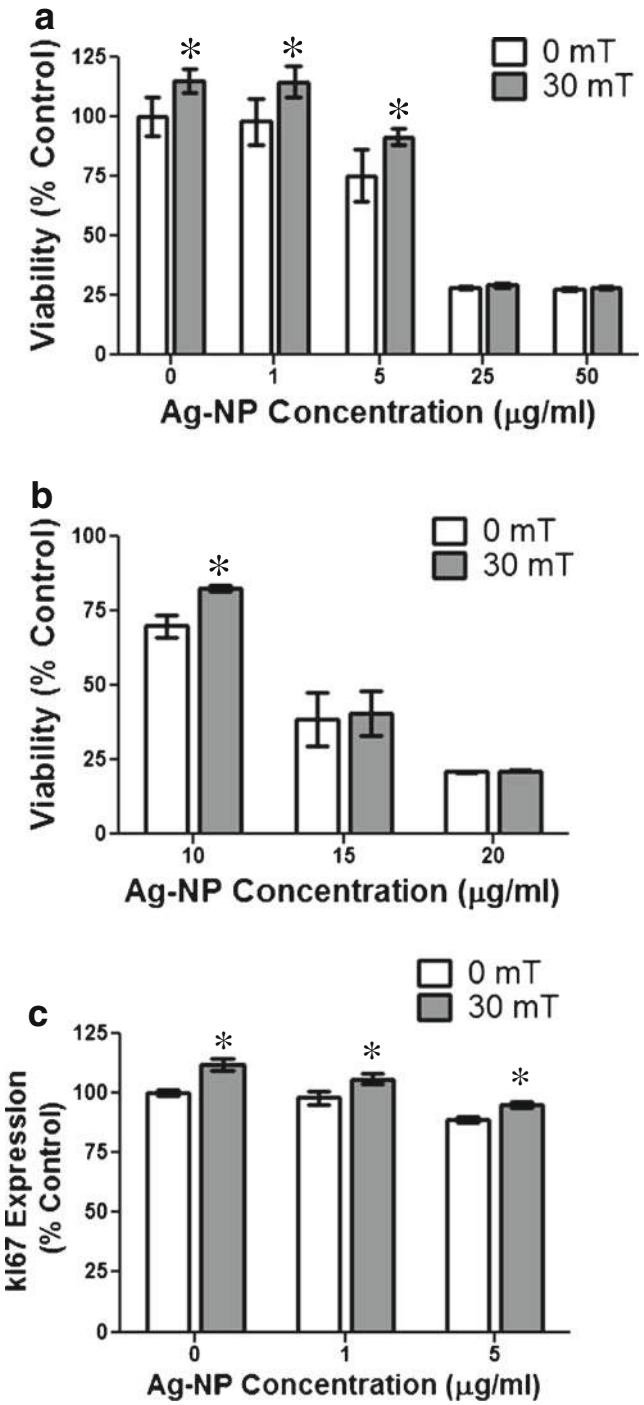

Fig. 4 NE-4C viability response during co-stimulation with AgNPs and a static MF. NE-4C cells were exposed to a 30 mT static magnetic field for 24 h in conjunction with a combination of AgNP concentrations. **a** During a traditional dose–response assessment, the MF was able to partially recover AgNP induced cytotoxicity at lower dosages. **b** A breakpoint of 10 μg/mL was identified for the ability of the MF to produce a 15 % protective effect from AgNP induced cytotoxicity, above which the MF had no additional response. **c** Expression of ki67, a recognized marker of cellular proliferation, was assessed during joint AgNP and MF exposure to verify the MF-dependent proliferative response (*$p <$ 0.05, denotes significance from the same AgNP concentration with 0 mT exposure)

The application of the static MF resulted in a noticeable increase in ki67 expression, which aligns with the observed recovery of NE-4C viability following MF exposure. The static MF was able to increase the ki67 expression at all concentrations of AgNP, including the control group, thus verifying the proliferative and protective response of MF on the neural cell system.

3.4 Concurrent AgNP and MF Exposure on Cellular Stress Markers

The next task was to elucidate the cellular mechanism behind this observed MF-reliant viability recovery. As the cytotoxic potential of AgNPs has been strongly linked to an increase in cellular stress, ROS was the next endpoint examined [36]. ROS is a recognized marker of cellular stress and one of the first cellular responses following introduction of AgNPs [37]. Our results are in agreement with that finding as a significant amount of ROS was generated, in a dose-dependent fashion, following AgNP introduction (Fig. 5). Interestingly, when a static MF was applied, it resulted in an approximately 40 % reduction of ROS levels for AgNP concentrations ranging from 0 to 10 μg/mL. There was no MF-dependent effect at the highest concentration of 25 μg/mL along with a sharp decrease in ROS production associated with extensive cytotoxicity observed at this concentration. This reduction in ROS levels displayed excellent correlation with the previous viability assessment. For AgNP concentrations ranging from 0 to 10 μg/mL, a respective decrease in ROS levels and increase in cell survival were coupled with MF stimulation indicating the protective nature of a static MF against AgNP-dependent stress and toxicity responses. These results suggest that ROS reduction by the application of MF is likely a contributing factor to the observed recovery of NE-4C death.

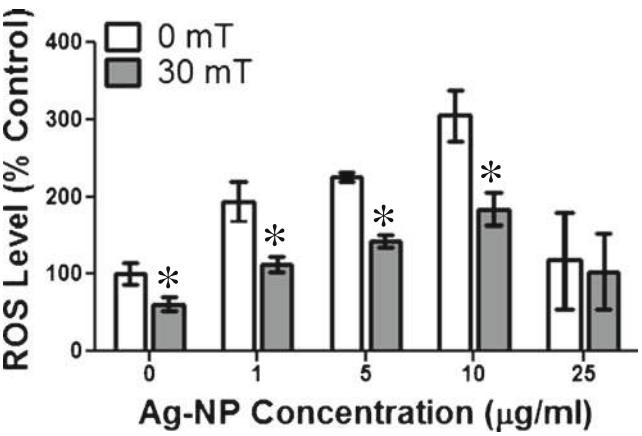

Fig. 5 Reduction in ROS levels by the application of MF. Exposure of NE-4C cells to AgNPs resulted in a dose-dependent increase in ROS production. However, cellular exposure to a 30 mT static MF was able to reduce the detected ROS levels by 40 % indicating a significant reduction in cellular stress (*$p < 0.05$, denotes significance from the same AgNP concentration with 0 mT exposure)

Additional analyses of the NE-4C stress response during co-exposure to AgNPs and a static MF was carried out to further elucidate the mechanism behind the observed recovery of cell viability. AgNPs were previously shown to induce the activation of the proteins c-Jun and NFκB, which are both involved in the nanosilver induction of cellular stress, inflammation, and apoptosis [38, 39]. In agreement with these previous results, our data indicated a dose-dependent increase in the expression of both c-Jun and NF-κB in response to AgNP exposure (Fig. 6). Interestingly, during joint AgNP and MF stimulation, the MF was able to partially reduce the c-Jun and NFκB activation in a similar fashion as previously seen with ROS. As these proteins are crucial players in cell death, a reduction in their expression correlates with and could potentially be a driving factor in the observed protective response of the static MF. Taken together, these results tell us that the MF is decreasing the amount of AgNP-induced stress endured by the NE-4C cells, as evaluated through ROS, c-Jun, and NFκB expression, thus allowing for more cellular growth and proliferation.

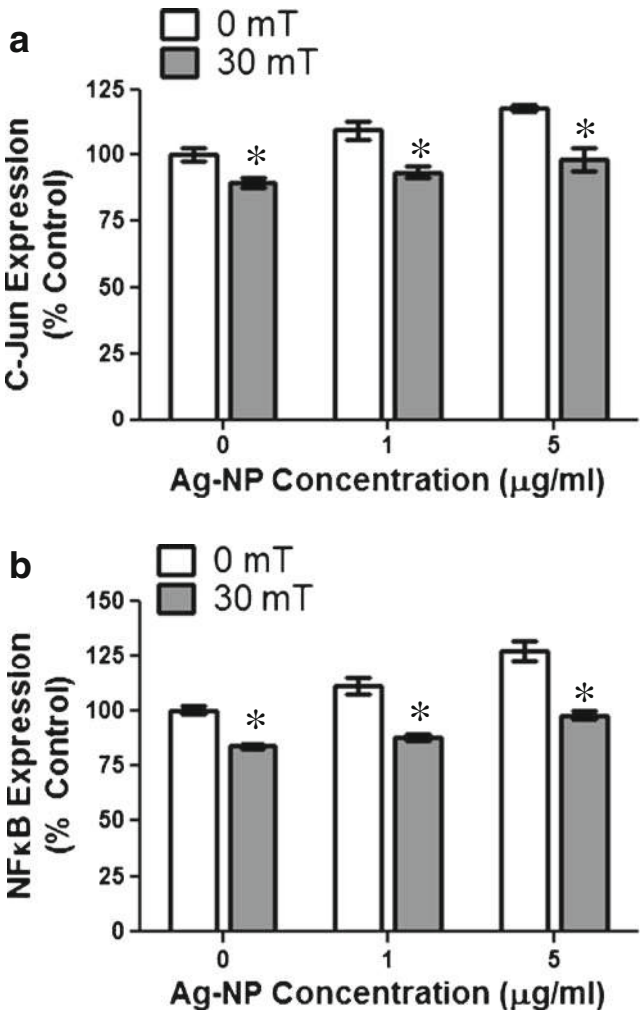

Fig. 6 Expression of stress markers in stimulated NE-4C cells. The expression levels of the stress and apoptotic markers **a** c-Jun and **b** NFκB were evaluated in the NE-4C cell line under the influence of AgNPs, a static MF, or both. Results demonstrated that the MF application was able to partially reduce the expression level of both proteins, thus reducing the cellular stress and cytotoxic responses (*$p < 0.05$, denotes significance from the same AgNP concentration with 0 mT exposure)

3.5 Quantification of Cellular AgNP Uptake

As the internalization rate of nanoparticles has been strongly linked to observed cytotoxicity [40], we sought to determine if application of MF impacted the degree of AgNP uptake by NE-4C cells. Following exposure to the static MF, the degree of AgNP internalization was reduced dramatically as seen in Fig. 7. After a 24-h exposure, the presence of MF was able to reduce the rate of AgNP internalization by approximately 50 %. MFs have been shown to increase uptake of magnetic nanoparticles typically for applications such as drug delivery and medical imaging [41, 42], but there is limited research analyzing the uptake of nonmagnetic nanoparticles under the influence of MF. One possible explanation for this response is that under the influence of MF, the NE-4C cells demonstrated an approximate 15 % increase in proliferation. Therefore, as the uptake is normalized by cell number, more cells existed, thus reducing the AgNP quantity per cells. However, this is likely to be only one factor contributing to this response. Another consideration is that nanomaterial size has been found to be a predominant factor in the degree of particle internalization [43]. However, as we previously demonstrated that the effective size was minimally altered by the MF, we concluded that size modification was not wholly responsible for this observed reduction in AgNP uptake, though a slight modification may have occurred due to this phenomenon.

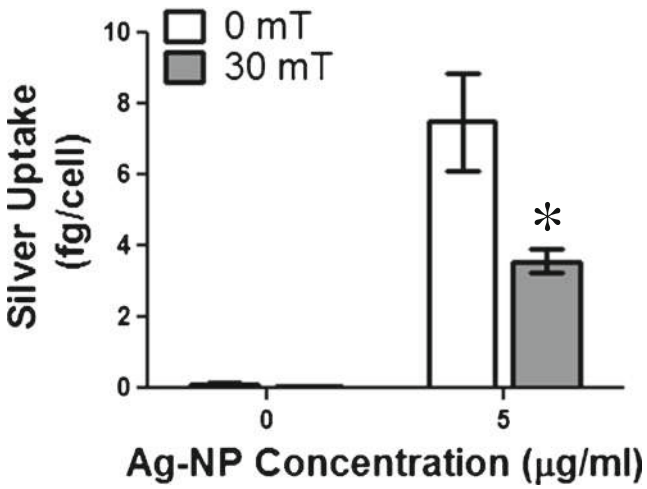

Fig. 7 Quantitative analysis of AgNP uptake in NE-4C cells. The influence of a static MF on the ability of NE-4C cells to internalize AgNPs was evaluated through ICP-MS. It was identified that the application of MF severely diminished the number of particles that were internalized after a 24 h time period (*$p < 0.05$, denotes significance from the same AgNP concentration with 0 mT exposure)

3.6 Identification of the Neuroprotective Ability of MFs

In recent history, a number of studies have explored the cellular implications of either AgNPs or MFs in an attempt to elucidate the resultant effects as a function of specific variables. Generally speaking, AgNPs have been found to induce a strong apoptotic response brought on by excess cellular stress and activation of the inflammatory response [44]. However, resultant MF bioeffects have been notoriously unpredictable but one fact that has remained constant is the fact that the stress response is a target of MF stimulation. Only a select few studies have explored the possibility of combinatorial bioeffects [23, 24], with results again indicating that cell proliferation and stress responses are key cellular targets during joint exposure. This raised the question if the application of MF would be able to diminish the negative responses associated with cytotoxic nanoparticles, such as AgNPs. Furthermore, a neural model appeared to be the optimal cellular system to target as it is most susceptible to stress fluctuations and a majority of pathologies are initiated by a disruption of stress homeostasis [15, 16].

In this study, we identified that the presence of a 30 mT static MF was able to provide a degree of protection to the neural NE-4C cell line following exposure to AgNPs at low dosages. This was supported by an approximate 15 % recovery of cell viability, which was brought on by a simultaneous increase in the expression of the proliferative ki67 protein and decrease in known stress markers ROS, c-Jun, and NFκB. However, it was found that this neuroprotective MF ability was only applicable at low AgNP concentrations, up to and including 10 μg/mL, after which the stress response was too large to be overcome by MF stimulation. Minimal alterations were noted in the AgNP characterization assessments after the addition of the MF, indicating that the particle properties and behavior were not the cause behind this response. Furthermore, no discernible MF-dependent differences were identified in evaluation of the nanocellular interface, supporting the hypothesis that this protective effect is brought on by a combinatorial bioeffect as a result of costimulation and not as a result of modifications to the particles themselves.

Most interestingly, the application of the static MF resulted in a 50 % reduction of AgNP internalization by NE-4C cells. Degree of cellular internalization has been strongly correlated to cellular death in a cellular system due to augmented ROS generation, pro-inflammatory cytokine secretion, and loss of mitochondrial function [45]. These results pose an intriguing question as to whether this decrease in AgNP uptake is responsible for the MF-dependent recovery of NE-4C viability observed or whether intracellular alterations activated by MF stimulation result in diminished rates of endocytosis. Nanoparticle endocytosis is strongly reliant on physicochemical parameters [46] and our characterization assessment identified only a minimal (~10 %) increase in AgNP agglomerate size during MF exposure. However, we do not believe that this small increase in effective AgNP size would produce such a pronounced drop in rate of internalization. Alternatively, we believe that when under the influence of MF, the NE-4Cs selectively choose to spend their energy stores on the proliferative and anti-apoptotic responses identified in this study. As both proliferation and endocytosis are energy dependent and an equivalent proliferative response of NE-4Cs to MF was observed in the absence of AgNPs, we believe that, taken together, this suggests that the cellular energy stores are being implemented to promote cell growth and development over endocytosis pathways.

4 Conclusions

AgNPs are rapidly gaining popularity in applications in both consumer and medical industries, causing concern over their documented detrimental cellular effects through increased stress responses and losses in viability. In this study, we demonstrated that the application of a 30 mT static MF was able to partially counteract these AgNP negative effects up to a certain concentration threshold. The rescue of cell viability was confirmed with increased ki67 expression and induced by a significant decrease in the NE-4C stress response including ROS generation and expression of c-Jun and NFκB. Furthermore, 30 mT MF did not impact AgNP behavior or the nanocellular interface, but did result in a 50 % drop in AgNP rate of endocytosis, possibly due to a redirection of energy stores toward proliferation. In conclusion, this study identified static MF stimulation as a possible mechanism to partially counteract the detrimental side-effects associated with AgNP exposure in a neural model. This opens up the possibility of including MF applications during nanobased neurological and biological applications as a means to control unintentional cellular consequences and improve application efficiency.

Acknowledgments The authors would like to thank Ms. Elizabeth Maurer TEM imaging and ICP-MS analysis and Ms. Emily Breitner for assistance with CytoViva imaging. NJB was supported through the Repperger Research Intern Program funded through the Air Force Chief Scientist's Office. KKC received funding from the Summer Faculty Fellowship Program supported by the Air Force Office of Scientific Research.

References

1. Kim, J. S., Kuk, E., Yu, K. N., Kim, J. H., Park, S. J., Lee, H. J., et al. (2007). Antimicrobial effects of silver nanoparticles. *Nanomedicine Nanotechnology, 3*, 95–101.
2. Quadros, M. E., & Marr, L. C. (2011). Silver nanoparticles and total aerosols emitted by nanotechnology-related consumer spray products. *Environmental Science and Technology, 45*, 10713–10719.

3. Wijnhoven, S. W. P., Peijnenburg, W., Herberts, C. A., Hagen, W. I., Oomen, A. G., Heugens, E. H. W., et al. (2009). Nano-silver—a review of available data and knowledge gaps in human and environmental risk assessment. *Nanotoxicol, 3*, 109–138.
4. AshaRani, P. V., Mun, G. L. K., Hande, M. P., Valiyaveettil, S. (2009). Cytotoxicity and genotoxicity of silver nanoparticles in human cells. *ACS Nano, 3*, 279–290.
5. Hussain, S. M., Hess, K. L., Gearhart, J. M., Geiss, K. T., Schlager, J. J. (2005). In vitro toxicity of nanoparticles in BRL 3A rat liver cells. *Toxicol in Vitro, 19*, 975–983.
6. Lee, K. J., Nallathamby, P. D., Browning, L. M., Osgood, C. J., Xu, X. H. N. (2007). In vivo imaging of transport and biocompatibility of single silver nanoparticles in early development of zebrafish embryos. *ACS Nano, 1*, 133–143.
7. Comfort, K. K., Maurer, E. I., Braydich-Stolle, L. K., Hussain, S. M. (2011). Interference of silver, gold, and iron oxide nanoparticles on epidermal growth factor signal transduction in epithelial cells. *ACS Nano, 5*, 10000–10008.
8. Singh, N., Manshian, B., Jenkings, G. J. S., Griffiths, S. M., Williams, P. M., Maffeis, T. G. G., et al. (2009). NanoGenotoxicology: the DNA damaging potential of engineered nanomaterials. *Biomaterials, 30*, 3891–3914.
9. Wan, R., Mo, Y. Q., Feng, L. F., Chien, S. F., Tollerud, D. J., Zhang, Q. W. (2012). DNA damage caused by metal nanoparticles: involvement of oxidative stress and activation of ATM. *Chemical Research in Toxicology, 25*, 1402–1411.
10. Mueller, N. C., & Nowack, B. (2008). Exposure modeling of engineered nanoparticles in the environment. *Environmental Science and Technology, 42*, 4447–4453.
11. Beer, C., Foldbjerg, R., Hayashi, Y., Sutherland, D. S., Autrup, H. (2012). Toxicity of silver nanoparticles—nanoparticle or silver ion? *Toxicology Letters, 208*, 286–292.
12. Kim, J., Kim, S., Lee, S. (2011). Differentiation of the toxicities of silver nanoparticles and silver ions to the Japanese medaka (*Oryzias latipes*) and the cladoceran *Daphnia magna*. *Nanotoxicology, 5*, 208–214.
13. Trickler, W. J., Lantz, S. M., Murdock, R. C., Schrand, A. M., Robinson, B. L., Newport, G. D., et al. (2010). Silver nanoparticle induced blood–brain barrier inflammation and increased permeability in primary rat brain microvessel endothelial cells. *Toxicological Sciences, 118*, 160–170.
14. Trickler, W. J., Lantz, S. M., Murdock, R. C., Schrand, A. M., Robinson, B. L., Newport, G. D., et al. (2011). Brain microvessel endothelial cells responses to gold nanoparticles: in vitro pro-inflammatory mediators and permeability. *Nanotoxicol, 5*, 479–492.
15. Saplosky, R. M. (2004). Stress and cognition. In M. S. Gazzaniga (Ed.), *Cognitave Neurosciences III* (3rd ed., pp. 1031–1042). New York, NY: Norton.
16. Sotiropoulos, I., Cerqueira, J. J., Catania, C., Takashima, A., Sousa, N., Almeida, O. F. X. (2008). Stress and glucocorticoid footprints in the brain—the path from depression to Alzheimer's disease. *Neuroscience Behavioral Review, 32*, 1161–1173.
17. Dini, L., & Abbro, L. (2005). Bioeffects of moderate-intensity static magnetic fields on cell cultures. *Micron, 36*, 195–217.
18. Miyakoshi, J. (2005). Effects of static magnetic fields at the cellular level. *Progress in Biophysics and Molecular Biology, 87*, 213–223.
19. De Nicola, M., Cordisco, S., Cerella, C., Albertini, M. C., D'Alessio, M., Accorsi, A., et al. (2006). Magnetic fields protect from apoptosis via redox alteration. *Annals of the New York Academy of Sciences, 1090*, 59–68.
20. Polidori, E., Zeppa, S., Potenza, L., Martinelli, C., Colombo, E., Casadei, L., et al. (2012). Gene expression profile in cultured human umbilical vein endothelial cells exposed to a 300 mT static magnetic field. *Bioelectromagnetics, 33*, 65–74.
21. Heinrich, A., Szostek, A., Nees, F., Meyer, P., Semmler, W., Flor, H. (2011). Effects of static magnetic fields on cognition, vital signs, and sensory perception: a meta-analysis. *Journal of Magnetic Resonance, 34*, 758–763.
22. Bae, J. E., Huh, M. I., Ryu, B. K., Do, J. Y., Jin, S. U., Moon, M. J., et al. (2011). The effect of static magnetic fields on the aggregation and cytotoxicity of magnetic nanoparticles. *Biomaterials, 32*, 9401–9414.
23. Comfort, K. K., Maurer, E. I., Hussain, S. M. (2013). The biological impact of concurrent exposure to metallic nanoparticles and a static magnetic field. *Bioelectromagnetics*. doi:10.1002/bem.21790.
24. Schafer, R., Bantleon, R., Kehlbach, R., Siegel, G., Wiskirchen, J., Wolburg, H., et al. (2010). Functional investigations on human mesenchymal stem cells exposed to magnetic fields and labeled with clinically approved iron nanoparticles. *BMC Cell Biology, 11*, 17.
25. Braydich-Stolle, L. K., Castle, A. B., Maurer, E. I., Hussain, S. M. (2012). Advantages of using imaged-based fluorescent analysis for nanomaterial studies. *Nanoscience Methods, 1*, 137–151.
26. Hussain, S. M., Braydich-Stolle, L. K., Schrand, A. M., Murdock, R. C., Yu, K. O., Mattie, D. M., et al. (2009). Toxicity evaluation for safe use of nanomaterials: recent achievements and technical challenges. *Advanced Material, 21*, 1549–1559.
27. Chithrani, B. D., Ghazani, A. A., Chan, W. C. W. (2006). Determining the size and shape dependence of gold nanoparticle uptake into mammalian cells. *Nano Letters, 6*, 662–668.
28. Murdock, R. C., Braydich-Stolle, L., Schrand, A. M., Schlager, J. J., Hussain, S. M. (2008). Characterization of nanomaterial dispersion in solution prior to in vitro exposure using dynamic light scattering technique. *Toxicological Sciences, 101*, 239–253.
29. Lynch, I., Salvati, A., Dawson, K. A. (2009). Protein–nanoparticle interactions: what does the cell see? *Nature Nanotechnology, 4*, 546–547.
30. Walkey, C. D., & Chan, W. C. W. (2012). Understanding and controlling the interaction of nanomaterials with proteins in a physiological environment. *Chemical Society Reviews, 41*, 2780–2799.
31. Chung, T. H., Wu, S. H., Yao, M., Lu, C. W., Lin, Y. S., Hung, Y., et al. (2007). The effect of surface charge on the uptake and biological function of mesoporous silica nanoparticles 3T3-L1 cells and human mesenchymal stem cells. *Biomaterials, 28*, 2959–2966.
32. Chionna, A., Tenuzzi, B., Panzarini, E., Dwikat, M. B., Abbro, L., Dini, L. (2005). Time dependent modifications of Hep G2 cells during exposure to static magnetic fields. *Bioelectromagnetics, 26*, 275–286.
33. Sakai, J., Li, J. Y., Subramanian, K. K., Mondal, S., Bajrami, B., Hattori, H., et al. (2012). Reactive oxygen species-induced actin glutathionylation controls actin dynamics in neutrophils. *Immunity, 37*, 1037–1049.
34. Tenuzzo, B., Chionna, A., Panzarini, E., Lanubile, R., Tarantino, P., di Jeso, B., et al. (2006). Biological effects of 6 mT static magnetic fields: a comparative study in different cell types. *Bioelectromagnetics, 27*, 560–577.
35. Scholzen, T., & Gerdes, J. (2000). The Ki-67 protein: from the known and the unknown. *Journal of Cell Physiology, 182*, 311–322.
36. Carlson, C., Hussain, S. M., Schrand, A. M., Braydich-Stolle, L. K., Hess, K. L., Jones, R. L., et al. (2008). Unique cellular interaction of silver nanoparticles: size-dependent generation of reactive oxygen species. *Journal of Physical Chemistry B, 112*, 13608–13619.
37. Fiers, W., Beyaert, R., Declercq, W., Vandenabeele, P. (1991). More than one way to die: apoptosis, necrosis, and reactive oxygen damage. *Oncogene, 18*, 7719–7730.
38. AshaRani, P. V., Sethu, S., Lim, H. K., Balaji, G., Valiyaveettil, S., Hande, M. P. (2012). Differential regulation of intracellular factors mediating cell cycle, DNA repair, and inflammation following exposure to silver nanoparticles in human cells. *Genome Integrity, 3*, 2.
39. Pioa, M. J., Kang, K. A., Lee, I. K., Kim, H. S., Kim, S., Choi, J. Y., et al. (2011). Silver nanoparticles induce oxidative cell damage in

human liver cells through inhibition of reduced glutathione and induction of mitochondria-involved apoptosis. *Toxicology Letters, 201*, 92–100.
40. Johnston, H. J., Hutchinson, G., Christensen, F. M., Peters, S., Hankin, S., Stone, V. (2010). A review of the in vivo and in vitro toxicity of silver and gold particulates: particle attributes and biological mechanisms responsible for the observed toxicity. *Critical Reviews in Toxicology, 40*, 328–346.
41. Dejardin, T., de la Fuente, J., del Pino, P., Furlani, E. P., Mullin, M., Smith, C. A., et al. (2011). Influence of both a static magnetic field and penetratin on magnetic nanoparticle delivery into fibroblasts. *Nanomedicine, 6*, 1719–1731.
42. Min, K. A., Shin, M. C., Yu, F. Q., Yang, M. Z., David, A. E., Yang, V. C., et al. (2013). Pulsed magnetic field improves the transport of iron oxide nanoparticles through cell barriers. *ACS Nano, 7*, 2162–2171.
43. Canton, I., & Battaglia, G. (2012). Endocytosis at the nanoscale. *Chemical Society Reviews, 41*, 2718–2739.
44. de Lima, R., Seabra, A. B., Durán, N. (2012). Silver nanoparticles: a brief review of cytotoxicity and genotoxicity of chemically and biogenically synthesized nanoparticles. *Journal of Applied Toxicology, 32*, 867–879.
45. Aillon, K. L., Xie, Y., El-Gendy, N., Berkland, C. J., Forrest, M. L. (2009). Effects of nanomaterial physicochemical properties on in vivo toxicity. *Advanced Drug Delivery Reviews, 61*, 457–466.
46. Frölich, E. (2012). The role of surface charge in cellular uptake and cytotoxicity of medical nanoparticles. *International Journal of Nanomedicine, 7*, 5577–5591.